Modeling and validation of polyurethane based passive underwater acoustic absorber

V. G. Jayakumari, Rahna K. Shamsudeen, R. Ramesh, and T. Mukundan[a)]
Naval Physical and Oceanographic Laboratory, Defense Research and Development Organisation, Thrikkakara, Kochi-686021, Kerala, India

(Received 2 August 2010; revised 8 June 2011; accepted 8 June 2011)

The acoustic behavior of an acoustically transparent polyurethane and an interpenetrating polymer network of polyurethane with polydimethyl siloxane were studied using dynamic mechanical analysis, finite element modeling, and experimental evaluation of acoustic properties in a water-filled pulse tube setup. Dynamic mechanical measurements in the temperature range −50 °C to +70 °C were carried out, and the data were used for time temperature superposition to generate material behavior at high frequencies. These inputs were used for modeling the acoustic behavior of these materials using ATILA, which is a commercial finite element code, capable of computing transmission and reflection characteristics of materials. From this data, absorption characteristics were computed. The results were compared with the experimental results obtained using a water-filled pulse tube facility. © *2011 Acoustical Society of America*. [DOI: 10.1121/1.3605670]

PACS number(s): 43.30.Ky, 43.35.Mr, 43.55.Ev [FCS] Pages: 724–730

I. INTRODUCTION

Materials that efficiently dissipate a substantial portion of the acoustic intensity of a propagating wave are in general known as attenuating materials. Such materials are essential for providing a stealth coating for ships and submarines. Also they are useful for anechoic lining of water filled tank facilities used for calibration and evaluation of underwater acoustic devices. It is important to develop damping materials suitable for these applications.[1–4] In many situations, the maximum damping obtainable with a single material may not be sufficient; rather a combination of different layers of materials is required. Several methods are employed to improve the damping capacities of polymers. Interpenetrating polymer networks (IPNs) are a class of polymers that are reported to give a broad range of damping.[5,6] These are materials with microheterogenous morphology and are different from polymer blends or composites. The loss modulus peaks characteristic of the individual polymers merge in an IPN and result in a broad band of frequencies over which a higher loss modulus is observed. This has been one of the common techniques used by researchers to broaden the effective damping range of polymers. However, for the purpose of underwater acoustic attenuation, the material should be compatible with water in terms of the acoustic impedance. Use of multilayer absorbers has become increasingly important in noise abatement.[7–9] This is particularly so in situations wherein damping a broad range of frequencies is essential.

To cater to futuristic requirements for underwater materials and to design and evaluate them, an ability to model and predict performance of different configurations is essential. Modeling can afford theoretical optimization of performance with respect to material configurations, thickness of different graded layers, and effect of size and concentration of various fillers. For a multilayer absorber development, this approach will enable low cost manufacturing of high performance materials leading to new structures and devices.[10–12]

In the present work, an acoustically transparent polyurethane (EPU) and its interpenetrating polymer network with polydimethyl siloxane (PDMS) were used. Acoustic behavior of these materials was modeled using ATILA, a commercial finite element modeling (FEM) code developed by ISEN, Lille, France.[13] The modeling results were compared with the experimental results obtained using a water-filled pulse tube facility.

II. EXPERIMENTAL

A. Materials

Raw material components of an EPU were received from Rand Polyproducts, Pune, India, and the silicone raw materials were from M/s Anabond Ltd., Chennai, India. For EPU, the resin: hardener ratio was kept at 100:40. The materials were mixed thoroughly and degassed for about 2 min to remove air bubbles, trapped during mixing. This polyurethane (PU) was cured at room temperature after pouring into a mold. This PU is designated as EPU in this study.

For realizing the IPN, PDMS components, Anabond 1217 A, B, and C were mixed according to predetermined compositions (97:3:6). This was reacted with PU prepolymers at room temperature with proper mixing. The PDMS: EPU composition was fixed at 1:1. The IPN was formed as a result of the simultaneous room temperature polymerization of both PDMS and EPU components.

a)Author to whom correspondence should be addressed. Electronic mail: t_mukun@yahoo.com; ms_npol@yahoo.co.in

 0001-4966/2011/130(2)/724/7/$30.00

The material densities were measured using a densimeter model Mirage MD 200 S (A & D Company Ltd, Tokyo, Japan).

B. Dynamic mechanical measurements

Dynamic mechanical testing is a versatile and sensitive tool enabling complete exploration of relaxational mechanisms in viscoelastic materials such as plastics and rubbers. The technique consists of applying a dynamic displacement to a specimen and measuring the force transmitted through the specimen. Dynamic mechanical analyzer (DMA, Q 800 model, TA Instruments, New Castle, DE) was used for dynamic mechanical measurements. The test mode, the specimen geometry and dimensions, and the measured stiffness allow calculation of various moduli, viz., complex modulus (E^*), storage modulus (E') and loss modulus (E'') of the material. The loss tangent, tan δ, which is the ratio of E'' to E', is also obtained.

It is well known that linear viscoelastic behavior of amorphous polymers and elastomers obeys the time–temperature superposition (TTS) principle.[14,15] This principle states that characteristic viscoelastic functions measured at different temperatures may be superimposed by parallel shifts along time or frequency axis. This helps to broaden the choice of frequency range using data obtained from experiments at various temperatures over a limited frequency range. The William–Landel–Ferry (WLF) equation[14,16] is typically used to describe the time–temperature behavior of polymers in the glass transition region (temperature at which transition from glassy to rubbery stage occurs; denoted as T_g). In the transition zone (T_g to $T_g + 50\,^{\circ}\mathrm{C}$), the WLF superposition principle generally applies to many polymers. The WLF equation is

$$\log a_T = \frac{-C_1(T - T_r)}{C_2 + (T - T_r)}, \tag{1}$$

where a_T is the shift factor, T_r is the reference temperature, C_1 and C_2 are constants and their values at T_g are; $C_1 = 17.4$ and $C_2 = 51.6$.

Sample dimensions used for DMA measurements were 35 mm length, 12.75 mm width, and 3 mm thickness. The samples were scanned in the temperature range $-50\,^{\circ}\mathrm{C}$ to $+70\,^{\circ}\mathrm{C}$. The dynamic stress applied on the sample was sufficient to produce a dynamic strain of 15 μm. The tests were carried out at various frequencies, 0.5, 1, 2, 5, 10, 20, and 50 Hz with a $5\,^{\circ}\mathrm{C}$ step in the temperature range. The isotherms obtained were shifted with respect to a reference temperature of $30\,^{\circ}\mathrm{C}$ with the help of TTS software. Once all the individual data points were shifted, a complete master curve for E', E'', or tan δ was obtained over an extended range of frequencies. During shifting, the shift factors obtained were stored by the computer as a function of temperature. WLF equation [Eq. (1)] was selected to relate shift factors to temperature. The data collected over two decades of frequency can be transformed to cover nine decades of frequency using this technique. The viscoelastic parameters obtained were used for modeling the acoustic behavior of these materials using ATILA.

C. Acoustic measurements

Acoustic properties of the samples were measured using a water-filled pulse tube.[17,18] A plane wave of known pressure amplitude propagates along the axis of the pulse tube and meets the specimen at normal incidence. The incident wave is partially reflected at the interface, partially absorbed by the material, and partially transmitted through the thickness of the material, as described schematically in Fig. 1. The fractions of the incident acoustic signal that are transmitted and reflected are represented as transmission coefficient (TC) and reflection coefficient (RC) as defined by

$$\mathrm{TC} = 10\log(I_t/I_i) = 20\log(P_t/P_i), \tag{2}$$

and

$$\mathrm{RC} = 10\log(I_r/I_i) = 20\log(P_r/P_i), \tag{3}$$

where, I_t, I_r, and I_i are the intensities of the transmitted, reflected, and incident waves, and P_t, P_r, and P_i are the corresponding pressure amplitudes, respectively. The sum of intensities of transmitted, reflected, and absorbed signals is unity in the linear scale. The absorption coefficient (AC) is determined from the reflection and transmission coefficients[19,20] as $\mathrm{TC} + \mathrm{RC} + \mathrm{AC} = 1$.

The experimental setup for measurement of acoustic property using pulse tube included a transmitter section consisting of an impulse generator (HP 3314 A, Hewlett Packard, California) and a power amplifier L2 (Instruments Inc., California) along with a low pass band filter (B & K 2650, Brüel and Kjaer, Denmark) to prevent excitation of higher order modes in the tube. This excited a transducer specially designed for this experiment that is made up of two lead zirconate rings sandwiched between two metal masses. The transducer used has a resonance frequency above the frequency band of interest. This transducer is fitted at the bottom of the tube, and it generates a sound pulse that travels along the axis of the tube. A half sine wave was used to excite the transducer. Figure 2(a) shows a representative view of the excitation pulse in the time domain, and Fig. 2(b) shows the time domain view of received signal, showing multiple reflections in the received time domain. The first pulse reflected from the sample was selected for analysis

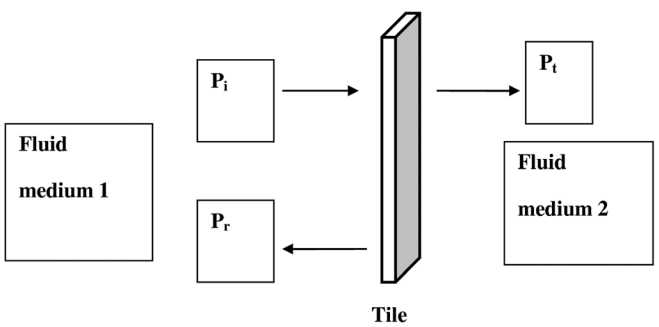

FIG. 1. Schematic of an acoustic wave propagating through a medium. For TC measurements, the fluid media 1 and 2 are water, and for RC measurements, fluid medium 1 is water and 2 is air. (Pi; incident sound pressure, Pt; transmitted sound pressure, Pr; reflected sound pressure).

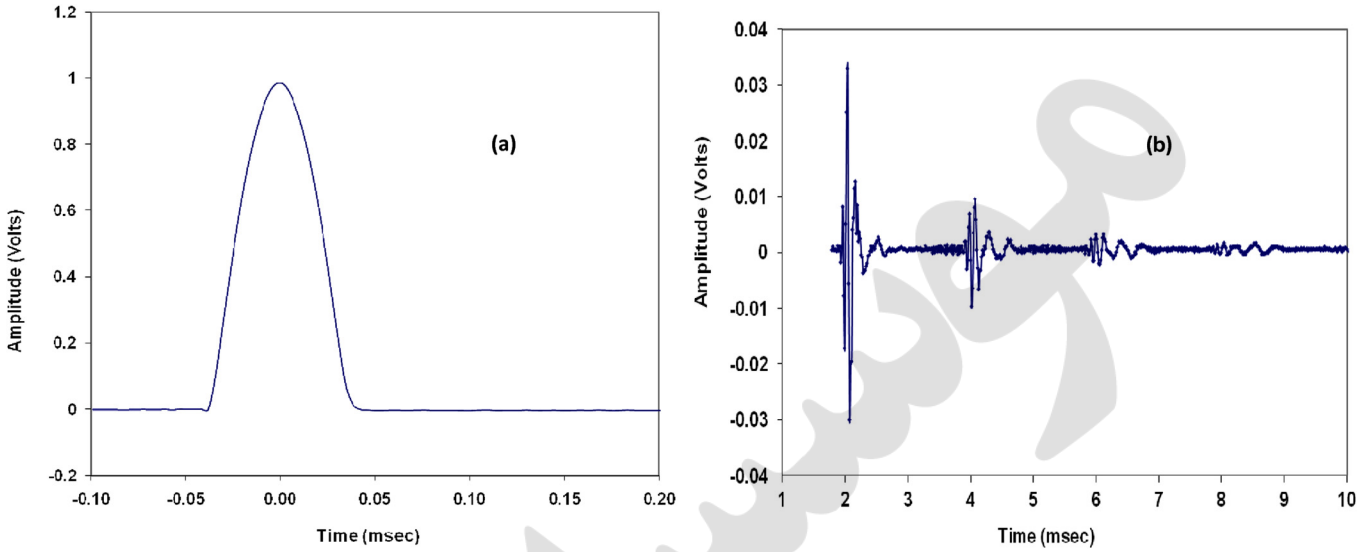

FIG. 2. (Color online) Time domain view of (a) representative input excitation pulse, (b) received output with multiple reflections.

using a built-in window function of the analyzer. A dynamic signal analyzer (HP 3562 A) was used for recording and for fast Fourier transform of received impulse signals and subsequent analysis.

The TC was measured from the pressure amplitudes of the incident wave and the wave transmitted to the other side of the sample, and the RC was measured from the pressure amplitudes of the incident wave and the wave reflected by the sample.

For TC measurements in the frequency range 1-4 kHz, a pulse tube of bore diameter 200 mm and length 4.8 m was used. The sample dimensions were 199 mm diameter and 10 mm thickness. The sample was positioned inside the tube at a depth of 2 m from the top through a single stranded nylon string. A probe hydrophone (B & K 8105) was positioned behind the sample to receive the transmitted signal through the test sample. After recording this transmitted signal, the sample was removed, and the hydrophone was positioned again to receive the signal in the absence of sample. From the signals received, TC was calculated using Eq. (2).

For RC measurements in the frequency range 2–15 kHz, a pulse tube of bore diameter 50 mm and length 1.48 m was used. The samples used were of 49.5 mm diameter and 25 mm thickness. The samples for RC measurements were pasted on the steel back plate of matching diameter the same as that of the sample, and 10 mm thickness, and was inserted into the tube from the top. The water layer on the top of the sample was removed carefully. The transducer was operated in the trans-receiver mode so that the same was used for generating the acoustic signal and also for receiving the reflected signal. After recording the reflected signal, the sample was removed, and the reflection from the water-air interface was measured. The ratio of these two measurements is the RC of the test sample as given in Eq. (3). A schematic for TC and RC measurements is shown in Fig. 3(a) and Fig. 3(b), respectively.

The dimensions of the pulse tube were decided by the method used and the frequency range of testing.[21,22] The pulse tube has an upper frequency limit dictated by its diameter. The plane wave exists up to this frequency, above which other modes are also generated. The measurement is restricted to plane wave propagation only. The upper frequency limit is calculated from the formula,

$$\mathrm{Freq}_{\mathrm{upper}} = 0.586^{*} c'/2r, \tag{4}$$

where c' is the speed of sound in the medium and r is the radius of the tube. The thickness of the tube was almost equal to that of the inner radius of the tube so that free field conditions are simulated inside the tube. The lower frequency limit possible for testing is determined by the length of the tube.

D. FEM

The FEM package ATILA was used for modeling the transmission and reflection characteristics of acoustic materials. Acoustic materials in the form of thin sheets were modeled. A plate that extends infinitely in the lateral dimensions but has finite thickness can be studied using ATILA by

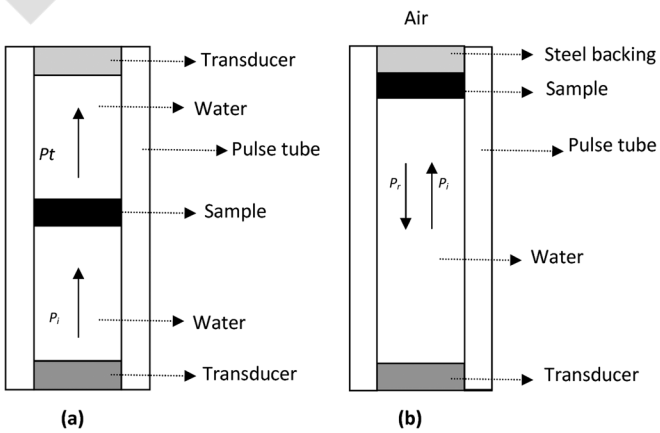

FIG. 3. Schematic of water-filled pulse tube setup for acoustic measurements (a) for TC measurements, (b) for RC measurements.

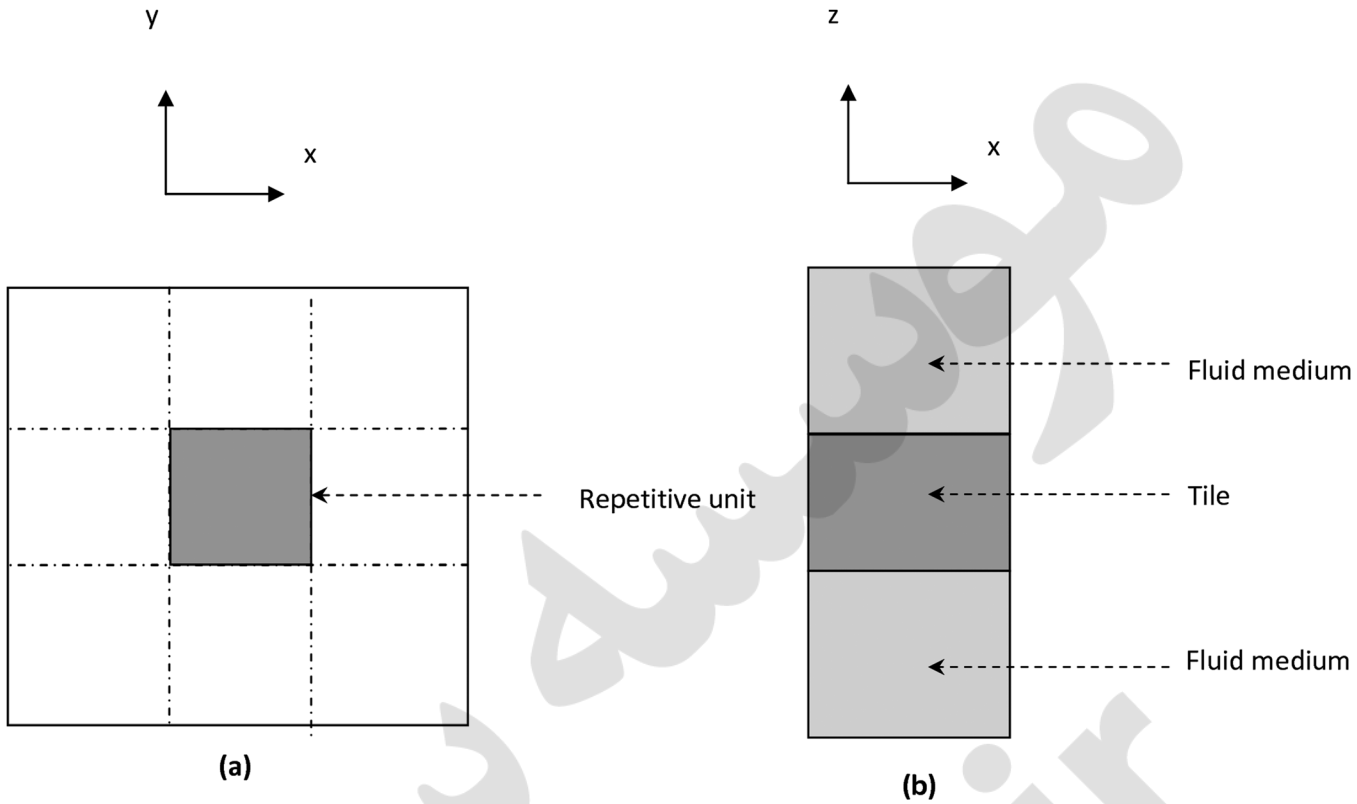

FIG. 4. Schematic diagram of the FE model of acoustic materials, (a) top view of one repetitive unit that is modeled and (b) front view of the vertical section of the model.

modeling a small portion of the material and applying periodic boundary conditions on the lateral sides. This significantly reduces the size of the problem and the computer memory requirements. A semi-infinite homogenous fluid medium, water or air, is included in the model on top and bottom sides. Acoustic plane waves of known amplitude and frequency are assumed to propagate in the positive z-direction from the fluid medium. The schematic of the acoustic material in the form of tiles considered in the present modeling study is shown in Fig. 4. The top view of one repetitive unit of the periodic structure taken for modeling is shown in Fig. 4(a), and the front view of the vertical section of the model with sample and adjacent fluid media is shown in Fig. 4(b). The fluid can be either water or air. The sample thickness is 10 mm for the water-tile-water model and 25 mm with 10 mm steel backing plate in the water-tile-air configuration to match the sample dimensions and configurations used in the experimental setup.

The model is divided into numerous small elements defined by the three-dimensional mesh. The mesh size of the various material components is maintained to be less than one-fifth of the highest wavelength in the respective materials as recommended by the ATILA user manual.[13] For fluids, IPN, EPU, and steel, 20-node hexahedral elements were used and for interfaces, 16-node quadrilateral elements were used. Periodic boundary conditions are applied on the adjacent sides to simulate the two-dimensional periodicity in the lateral directions (xy plane). Internal losses of the materials are accounted for in the analysis. The Young's modulus and loss parameter of IPN and EPU materials are frequency-dependent, and hence dynamic values are needed. The material parameters used in the modeling were obtained from DMA and subsequent time temperature superposition. Harmonic analysis is carried out at spot frequencies in the range 1–15 kHz, which is the range of interest for acoustic measurements in the present study.

III. RESULTS AND DISCUSSION

The experimentally obtained storage moduli, loss moduli (E' and E'', respectively), and tan δ values from DMA measurements for EPU and IPN as a function of temperature are shown in Figs. 5 and 6, respectively. Results show that

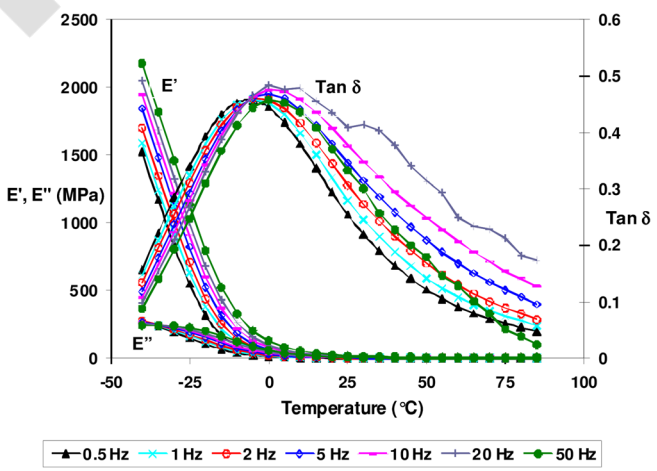

FIG. 5. (Color online) Dynamic mechanical analysis data of EPU.

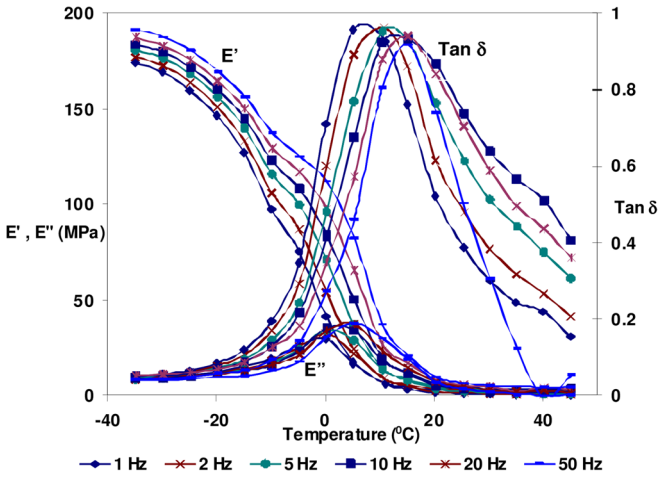

FIG. 6. (Color online) Dynamic mechanical analysis data of IPN.

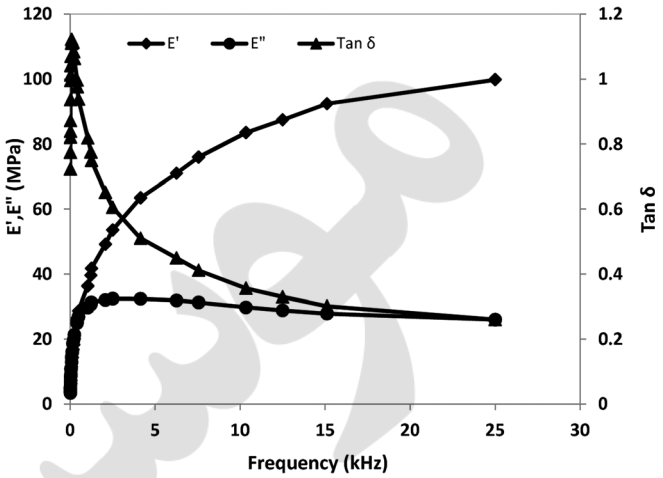

FIG. 8. Dynamic mechanical properties of IPN as predicted by time–temperature superposition.

EPU has low tan δ values (Fig. 5) and can be used as an acoustically transparent material. Figure 6 shows that tan δ of IPN is much higher, particularly in the low frequency region. The interpenetrating network structure provides domains of micro-heterogeneouss morphology, which helps in effective acoustic wave attenuation. IPN has a more soft and flexible nature as evidenced by low modulus values compared to EPU. Modulus at T_g is ~2000 MPa for EPU, whereas it is ~190 MPa for IPN resulting in high viscoelastic damping. Storage and loss modulus (E' and E'') of IPNs are small compared to EPU because the IPN material is more flexible.

These raw data were used for performing TTS and generating data at higher frequencies. Figures 7 and 8 show TTS predicted values of E', E'', and tan δ of EPU and IPN, respectively, in the frequencies up to 25 kHz. It is seen that loss modulus and tan δ values of IPN are more in the low frequency region (1–12 kHz) compared to EPU. This frequency region is particularly important for acoustic absorber panels used for underwater applications.[1] Figure 9 shows a comparison of the tan δ values of EPU and IPN in the frequency range 1–4 kHz. It can be seen that there is broadening as well as increase in the height of tan δ peak for IPN, whereas that of EPU is flat. This indicates better damping of IPN in the frequency range 1–4 kHz and hence its suitability for low frequency damping applications.

The inputs, E' and tan δ from Figs. 7 and 8 were used for modeling the acoustic behavior of EPU and IPN using ATILA. Apart from this, the other inputs required were density and Poisson's ratio of the materials. The densities of EPU and IPN were 1.1 and 0.99 g/cm^3, respectively, and the Poisson's ratio was assumed to be 0.48, which is a generic value for PU elastomers. For an acoustically transparent material like EPU, TC measurements are sufficient to characterize its acoustic behavior. Therefore, for EPU, a comparison of modeling and experimental results of TC was done. However, for an absorber material such as IPN, the RC measurements are more pertinent as far as the present method of measurements is concerned. For a configuration with air above the sample, total reflection of incident wave occurs due to the impedance mismatch between the sample/air interface and water (present in the annular gap)/air interface.

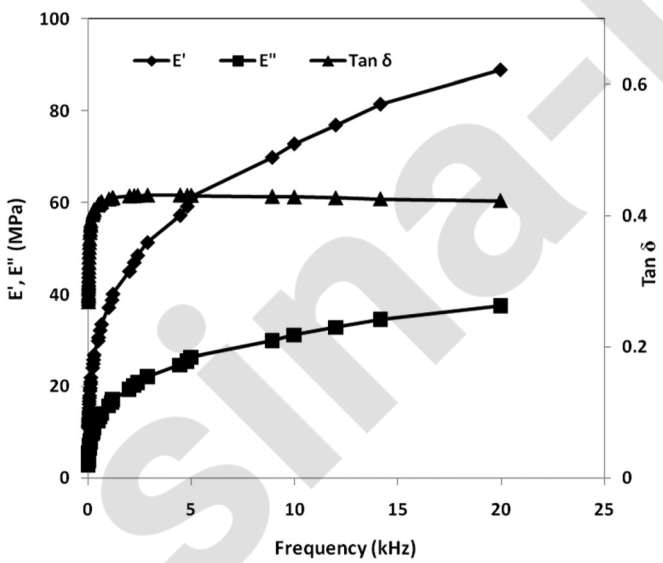

FIG. 7. Dynamic mechanical properties of EPU as predicted by time–temperature superposition.

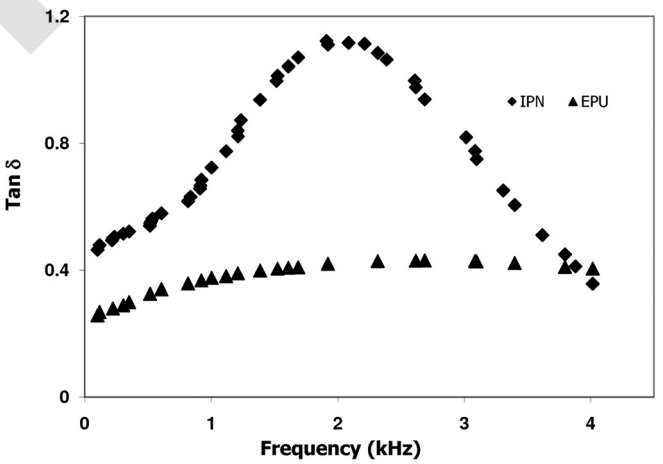

FIG. 9. Comparison of tan δ values for IPN and EPU materials predicted by time–temperature superposition in the frequency range 1–4 kHz.

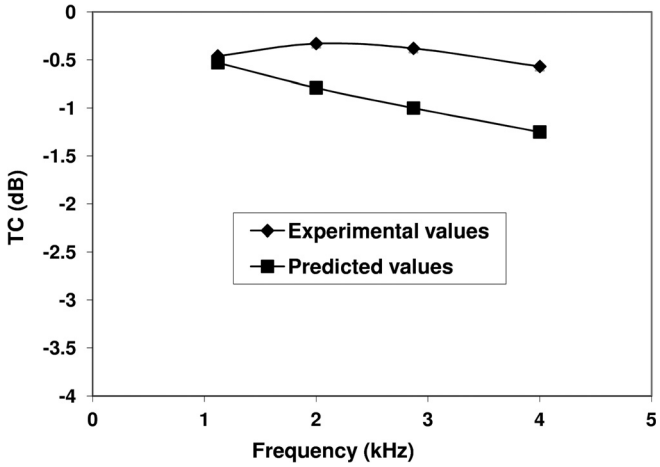

FIG. 10. Comparison of modeling and experimental results of EPU (water–tile–water configuration).

Hence, for IPN, a comparison of modeling and experimental results of RC was done. Modeling results were computed for each frequency independently.

Due to the limitation imposed by the pulse tube, experimental TC data could be obtained in the frequency range 1–4 kHz only. A comparison of these experimental results with modeling in 1–4 kHz range is shown in Fig. 10. The results clearly show that EPU is an acoustically transparent material in the stated frequency range. The experimental and modeling results match very well, within 1 dB, for transmission loss characteristics of EPU.

For the IPN, AC was calculated from TC and RC because the sum of all three coefficients is unity. The results are shown in Fig. 11. For the IPN, an absorption coefficient 5–8 dB was achieved. The configuration for modeling for all the above-described results was water–tile–water. (Both fluid medium 1 and 2 are water as per Fig. 1.)

To compare the RC values of IPN obtained experimentally and by modeling of IPN, a configuration, viz., water–tile–air (water is fluid medium 1 and air is fluid medium 2 as

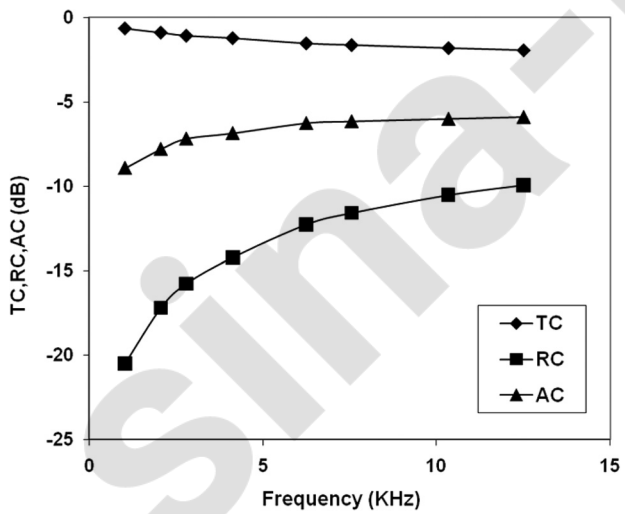

FIG. 11. Acoustic data of IPN from FEM modeling (water–tile–water configuration).

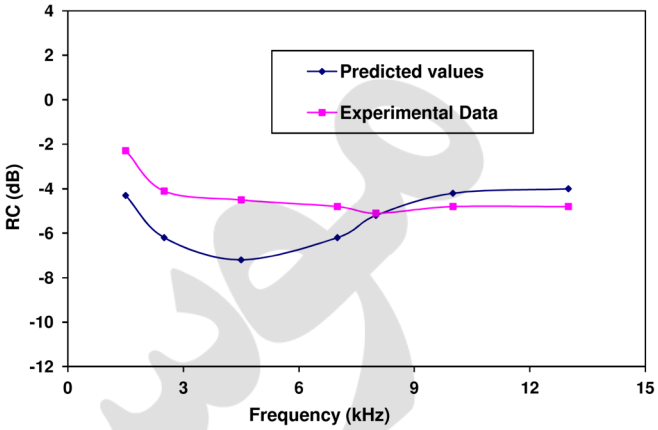

FIG. 12. (Color online) Comparison of modeling and experimental results for IPN (water–tile–air configuration).

per Fig. 1) is modeled, and the results are compared with the experimental values as shown in Fig. 12.

However, the results showed a maximum variation of ± 3 dB at certain frequencies that may be attributed to the microheterogeneous nature of IPN.

It was observed that modeling and experimental results match well for the acoustically transparent material in water–tile–water model, whereas for the IPN type of absorber materials, a deviation of experimental results from modeled results is obtained. In IPNs, different acoustic attenuation mechanisms such as scattering of acoustic waves, wave redirection, etc. may also operate due to the microheterogeneous nature of the material in addition to viscoelastic damping. This may be the reason for the observed deviation of the model result from the experimental value.

IV. CONCLUSION

Experimentally measured dynamic mechanical parameters were used in an FEM modeling program (ATILA) to calculate the high-frequency acoustic characteristics of the samples. The results were compared with acoustic measurements done in a water-filled pulse tube facility for validation. It was observed that for the acoustically transparent material (EPU), the experimental and modeling results match very well within 1 dB for transmission coefficient values. However, for absorber material (IPN), a maximum deviation of ± 3 dB was observed for the reflection coefficient values. The method described provides a route to predict performance of different acoustically transparent and absorber materials using FEM modeling. This can lead to theoretical optimization of performance with respect to material configurations, thickness of different graded layers, and effect of size and concentration of various fillers to enable low cost manufacturing of high performance materials leading to new structures and devices. Further studies on these lines are in progress for the design of multilayered absorbers.

ACKNOWLEDGMENTS

The authors thank the director of the Naval Physical and Oceanographic Laboratory (NPOL) for granting permission

to publish the work and the Transducer Group, NPOL for facilitating acoustic measurements for the present work.

[1]R. D. Corsaro and L. H. Sperling, *Sound and Vibration Damping with Polymers* (ACS Symposium Series, Washington, DC, 1990).
[2]Z. Hong, L. Bo, and H. Guangsu, "Sound absorption characteristics of polymer microparticles," J. Appl. Polym. Sci. **101**, 2675–2679 (2006).
[3]B. Philip, J. K. Abraham, V. K. Varadan, V. Natarajan, and V. G. Jayakumari, "Passive underwater acoustic damping materials with Rho-C rubber - carbon fiber and molecular sieves," Smart Mater. Struct. **13**, N99–N104 (2004).
[4]K. Urayama, T. Miki, T. Takigawa, and S. Kohjiya, "Damping elastomer based on model irregular networks of end-linked Poly (dimethyl siloxane)," Chem. Mater. **16**, 173–178 (2004).
[5]M. C. O. Chang, D. A. Thomas, and L. H. Sperling, "Sound and vibration damping with interpenetrating polymer networks," J. Polym. Mater. **6**, 61–72 (1989).
[6]R. Y. Ting, R. N. Capps, and D. Klempner, "Acoustical properties of some interpenetrating network polymers," in *Sound and Vibration damping with Polymers*, edited by R. D. Corsaro and L. H. Sperling (ACS Symposium Series, WA, 1990), Chap. 20, pp. 366–381.
[7]W. H. Chen, F. C. Lee, and D. M. Chiang, "On the acoustic absorption of porous materials with different surface shapes and perforated plates," J. Sound Vib. **237**, 337–355 (2000).
[8]F. C. Lee and W. H. Chen, "On the acoustic absorption of multilayer absorbers with different inner structures," J. Sound Vib. **259**, 761–777 (2003).
[9]F. Asdrubali, "Properties of transparent sound-absorbing panels for use in noise barriers," J. Acoust. Soc. Am., **121**(1), 214–221 (2007).
[10]S. N. Panigrahi, C. S. Jog, and M. L. Munjal, "Multi-focus design of underwater noise control linings based on finite element analysis," Appl. Acoust. **69**, 1141–1153 (2008).
[11]C. Cai, K. C. Hung, and M. S. Khan, "Simulation-based analysis of acoustic absorbent lining subject to normal plane wave incidence," J. Sound Vib. **291**, 656–680 (2006).
[12]D. Razansky, P. D. Einziger, and D. R. Adam, "Effectiveness of acoustic power dissipation in lossy layers," J. Acoust. Soc. Am. **116**(1), 84–89 (2004).
[13]ATILA "Finite element code for piezoelectric and magnetostrictive transducer modeling" (ISEN, Lille, France, 2010).
[14]J. D Ferry, *Viscoelastic Properties of Polymers* (Wiley, New York, 1980), pp. 287–290.
[15]P. T. Wiessman and R. P. Chartoff, "Extrapolating viscoelastic data in the temperature-frequency domain," in *Sound and Vibration Damping with Polymers*, edited by R. D. Corsaro and L. H. Sperling (ACS Symposium Series, WA, 1990), Chap. 7, pp 111–131.
[16]M. L. Williams, R. F. Landel, and J. D. Ferry, "The temperature dependence of relaxation mechanisms in amorphous and other glass forming liquids," J. Am. Chem. Soc. **77**, 3701–3707 (1955).
[17]R. J. Bobber, *Underwater Electroacoustic Measurements* (Peninsula Publishing, Los Altos, CA, 1988), pp. 287–314.
[18]L. Sun and H. Hou, "Transmission loss measurement of acoustic material using time-domain pulse separation method (L)," J. Acoust. Soc. Am. **129** (4), 1681–1684 (2011).
[19]L. E. Kinsler, A. R. Frey, A. B. Coppens, and J. V. Sanders, *Fundamentals of Acoustics* (Wiley, New York, 2000), pp. 149–166.
[20]H. T. Loeser, *Sonar Engineering Handbook* (Peninsula Publishing, Los Altos, CA, 1992), pp. 3.24–3.41.
[21]H. J. Sabine, "Notes on acoustic measurement," J. Acoust. Soc. Am. **13**, 143–149 (2004).
[22]E. Meyer, in *Technical Aspects of Sound*, edited by E. G. Richardson (Elseveir, New York, 1957), Vol. II, pp. 201–221.